Design and fabrication of a fast-response and low-energy input micro igniter

Tao Wu, Vidushi Singh, Baptiste Julien, Maria-Isabel Mendoza-Diaz, Fabien Mesnilgrente, Samuel Charlot, Carole Rossi

Design and fabrication of a fast-response and low-energy input micro igniter

Tao Wu[*], *Vidushi Singh, Baptiste Julien, Maria-Isabel Mendoza-Diaz, Fabien Mesnilgrente, Samuel Charlot, Carole Rossi*[*]

LAAS-CNRS, University of Toulouse, 7 Avenue du colonel Roche, 31400 Toulouse, France

Abstract

In this study, we innovatively combine direct ink writing (DIW) and physical vapor deposition (PVD) to fabricate a novel micro igniter with fast-response and low-energy input characteristics. The igniter comprises a 5×5 mm² metal film bridge with gold contact pads. The metallic resistance is fabricated using a series of photolithography, metal deposition, and lift-off processes. After evaluating titanium and chromium as the resistive filament, titanium was selected due to its superior reactivity when in contact with CuO leading to reduced ignition energy. Onto the resistive titanium layer, either thermite multilayer films and/or energetic inks are deposited to achieve a head-to-head comparison of ignition characteristics. We show that igniters powered by $(CuO/Ti)_5$ bilayers and Al/CuO/PVDF as energetic ink demonstrate the equivalent ignition performance as reactive $(CuO/Ti)_5$ multilayered igniter. The ignition delay and ignition energy are below 1 ms and 2 mJ, respectively, while the flash intensity is approximately one decade higher than what is typically achieved with conventional micro-igniters. Furthermore, its ignition behaviour can be readily adjusted by altering the constituents of the fuel/oxidizer or adjusting the ratio of multilayer/inks, thereby allowing for easy adaptation of the micro-igniter to meet the diverse requirements of various applications.

Keywords: MEMS, Igniters, Thin-films, direct ink writing, energetic materials.

1. Introduction

Pyrotechnics encompass a diverse array of sophisticated devices capable of generating heat, light, smoke, sound, motion, or a combination thereof [1–5]. These effects are achieved through the controlled reaction of highly energetic materials, including explosives, propellants, and pyrotechnic compositions.

[*] Corresponding author:
E-mail address: twu@laas.fr (T. Wu), rossi@laas.fr (C. Rossi),

Notably, pyrotechnic devices exhibit high efficiency, delivering substantial energy per unit weight, surpassing other actuation mechanisms. This efficiency allows for prompt energy release upon demand, even after extended periods of storage [6–9]. The applications of pyrotechnics span various industries, including defense, civil engineering, demolition, fireworks, automotive, and aerospace. Within these sectors, pyrotechnic devices serve diverse purposes, including initiation [1,10], actuation [11,12], severance/fracture [12–15], jettison/valving/switching [16,17], welding [18,19], and joining [20,21]. The only external energy required is an initiation trigger to set off the self-sustained combustion of the energetic materials. Most pyrotechnics utilize a simple hot wire (low resistance Ni-Cr filament) for initiating the energetic material reaction [22]. This low-voltage igniter heats the filament, leading to the auto-inflammation of a primary or secondary explosive such as a potassium perchlorate or nitrate. The technology is simple, inexpensive and reliable. Nevertheless, over the past two decades, efforts have been directed towards enhancements aimed at minimizing the footprint of igniters and enhancing their safety [23]. This involves replacing high explosive substances with non-hazardous and insensitive materials. Innovations like exploding foils or semiconductor bridge devices (SCB) [24–27] have been developed to initiate insensitive materials, thereby contributing to improved safety standards. These devices usually require very short durations and high-firing current and voltage (resulting in low total energy due to extremely short pulses). They generate a high-temperature plasma or shock wave output, meet the one amp/one watt (1 A/1 W)/5 min no-fire requirement, and exhibit tolerance to electrostatic discharge. With its superior ignition properties, including rapid response, low energy input, and high degree of integration, SCB has been largely employed in spatial and military applications. However, its application is limited by cost considerations and incompatibility with existing electronic microcircuits utilized in numerous civilian applications, like automotive or aeronautics. Indeed, the generation of high-temperature plasma for ignition in SCB typically demands a substantial power input, usually in the kilowatt (kW) range.

More recently, researchers have introduced a reactive metal film bridge (RMFB) as an alternative to the SCB allowing for adjustable electrical power and energy input by modifying the types and thickness of metals [28–33]. A typical RMFB comprises of a metallic thin film (such as Ni-Cr [22,34], Cr [35], Au-

Ti [26], Ti [28,30,31]) onto which a reactive multilayer film is deposited. This latter is composed of alternating nanolayers (tens to hundreds of nm) of metal (Al [29,36], Ti [30], TiB_2 [37,38]) and oxidizer (CuO [39,40], MoO_3 [27]). Aluminum is often the chosen metal for the reactive multilayer films due to its high availability, low cost and well-developed deposition process [29]. Meanwhile, CuO was selected as the oxidizer due to its relative stability in ambient conditions, its ease of sputter-deposition, and its known use as a reducing agent/oxygen source for thermite reactions [30,41]. Over the years, Al/CuO multilayers have gained interest due to their capability to promptly (in a time scale of µs) release a large amount of energy (up to 4 $kJ.g^{-1}$) in the sudden emission of light and heat [29,31]. However, the fabrication process, primarily relying on magnetron sputtering, a physical vapor deposition (PVD) technique [29,33] faces drawbacks. These include low mass loading, extended processing times, and issues such as delamination induced by residual stress. These challenges restrict the widespread sectors application of RMFB as an alternative of hotwire/bridge wire. Hence, there is a crucial demand for an alternative fabrication method to be developed that preserves the advantages and addresses the drawbacks of RMFB chip. We propose to take advantage of the direct ink writing (DIW) technique which has garnered significant attention in recent decades owing to its easy manipulation, low cost, high adaptability and scalability [42–44]. By studying both processes, we aim to develop a low-energy input and high-power micro-igniter, so called energetic MFB igniter.

The contribution of this paper is two-fold: 1) we develop a very efficient MFB igniter that achieves rapid ignition by employing titanium as the metal resistance and a mixture of Ti/CuO and Al/CuO multilayers as energetic layers; 2) we propose a solution that effectively balances ignition performance with the fabrication cost of micro-igniters, while maintaining high tunability in their ignition capabilities through adjustments in the thermite or multilayer/inks ratio.

2. Igniters fabrication process

This section describes the micro-fabrication process of a 5×5 mm^2 metal bridge igniter that is summarized in **Figure 1**. We utilized two different metals, namely chromium and titanium, as candidates to construct the resistance filament. Their thicknesses were adjusted to approximately 360 nm and 750 nm, respectively, to achieve an equivalent electrical resistance of approximately 2 Ω. In

detail, as the first step, a negative photoresist (NLOF2035, MicroChemicals, 5 µm) was spin-coated onto a clean glass wafer to obtain a 5 µm thick NLOF layer. This photoresist layer was soft baked at 105 °C for 1.5 min and cooled down to room temperature. The photoresist layer was subsequently patterned by exposing it to UV light (A6 Gen4 Suss Microtec, 150 mJ/cm²) through a contact mask that delineated the shape of the resistance and contact, as depicted in **Figure 1** – step 2. After a post-bake at 110 °C for 1.5 min, the pattern was then transferred to the photoresist layer by developing the exposed photoresist using a MF-CD-26 developer for 2 min, followed by rinsing in deionized water, and dried under N_2. Then, a Ti (720 ± 20 nm) or Cr (360 ± 10 nm) / Au (300 nm) bi-layer was sputter-deposited to obtain the resistance and contact layers (**Figure 1** – step 3). To remove the excess photoresist and reveal the metal film bridge structure, the wafer was put into an acetone bath for 3 h followed by another 10 min of sonication. After this step, we end up with Ti or Cr resistance layer at the bottom and contact Au layered on top, as shown in **Figure 1** – step 5.

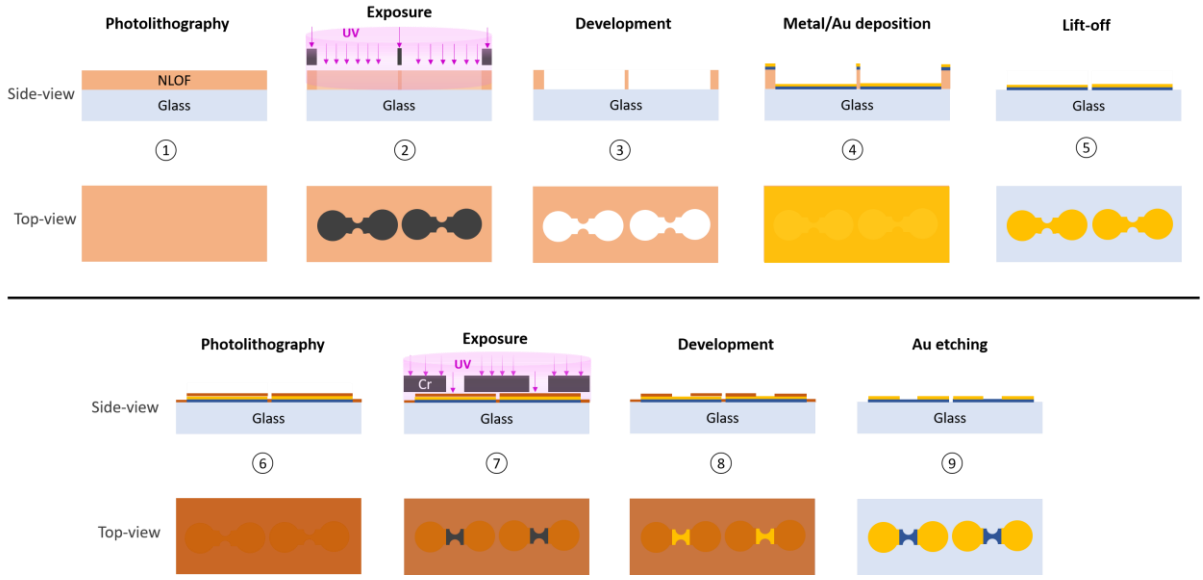

***Figure 1**. Process flow of MFB fabrication (zoomed on two resistances).*

To reveal the resistance filament, a second photolithography process was performed as presented in **Figure 1** – step 6. A positive photoresist (ECI-3012, MicroChemicals, 1 µm) was spin-coated onto a clean glass wafer to obtain a 1 µm thick ECI layer. This photoresist layer was soft baked at 90 °C for 60 s and cooled down to room temperature. The photoresist layer was then patterned by exposing it

under UV light (A6 Gen4 Suss Microtec, 200 mJ/cm²) through a contact mask defining the resistance shape, as indicated in **Figure 2** – step 7. After a post-bake at 110 °C for 60 s, the pattern was then transferred to the photoresist layer by developing the exposed photoresist using a MF-CD-26 developer for 20 s, followed by rinsing in deionized water, and dried under N_2. Then, the wafer was put in a gold etching solution composed of KI and I_2 for 90 s to remove the exposed gold layer; afterwards, the defined resistance is realized and revealed and the electrical resistance is measured to be at 2.2 ± 0.1 Ω for Ti and 1.9 ± 0.1 Ω for Cr. **Figure 2** gives a photo of one MFB chip thus fabricated. **Table 1** summarizes the measured resistance and film roughness. **Figure S1** shows the profilometer scans of both resistance filaments after deposition on glass wafer. We can clearly observe that the surface of the titanium thin film filament is considerably smoother than that of chromium. This smoother surface contributes to a more defined profile of the resistance, which is essential for maintaining uniformity in multilayer films during the fabrication of RMFB.

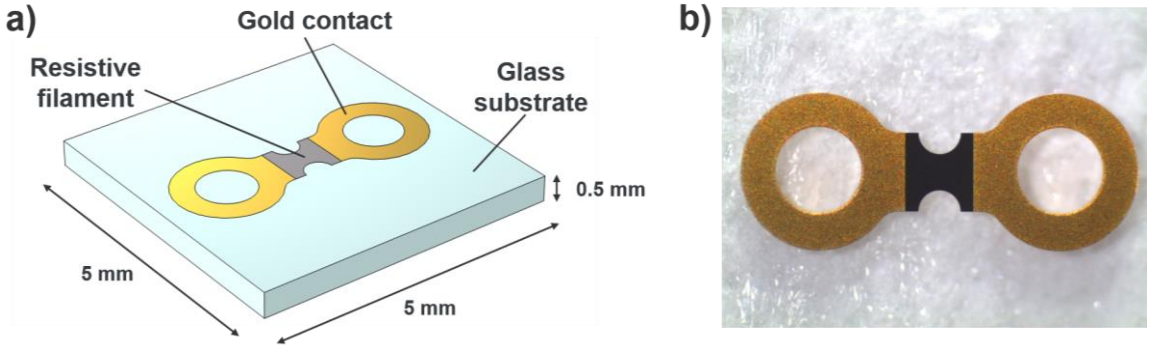

Figure 2. *A schematic (a) and digital image (b) of one MFB chip.*

Table 1*. Electrical resistance and roughness of the different resistance filament materials used in MFB devices.*

Metal	Resistance (Ω)	Roughness (nm)
Cr	1.9 ± 0.1	370 ± 50
Ti	2.2 ± 0.1	750 ± 5

Once the MFB is realized, a thermite is deposited onto it. Two distinct processes were employed as indicated in **Figure 3**: either by sputter-depositing reactive multilayer films, i.e. RMFB, or by depositing energetic Al/CuO/PVDF films by direct ink writing, i.e. energetic MFB (EMFB).

***Figure 3**. Schematics of the energetic layer deposition, by magnetron sputtering and direct ink writing, to achieve a high-energy and low-power MFB igniter.*

2.1. Sputter deposition of reactive multilayer films to fabricate the RMBF igniters

Approximately 12 mm² of CuO/Metal (Al or Ti) multilayer films are patterned and sputter-deposited onto the pre-deposited MFB igniter chip. Each of the nanolayers, CuO and Metal were sputter deposited using direct current magnetron sputtering with a tool from Thin Film Equipment (TFE), Italy, utilizing 8 by 3 square inches and ¼ inch thick targets from Neyco, France. For CuO nanolayer, the oxygen and argon gas flow were set to 19.2 and 32 cm^3/min with a partial pressure of 10^{-2} mbar. The Ar partial pressure during metal deposition was maintained at 5.10^{-3} mbar. The sample was cooled to ambient temperature for 600 s at the end of the deposition process. The thermite film always starts with 200 nm of CuO which is therefore in direct contact with the metal bridge filament (Ti or Cr). The individual Al, Ti, and CuO thickness is set at 200 nm, 170 nm, and 200 nm respectively, resulting in an equivalence ratio of 2:1 (fuel-rich configuration). Then the wafer is diced into individual RMFB chips. The **Figure 4** presents the look of a single chip and a SEM cross section image the 15 BL CuO/Al 200/200nm reactive multilayers.

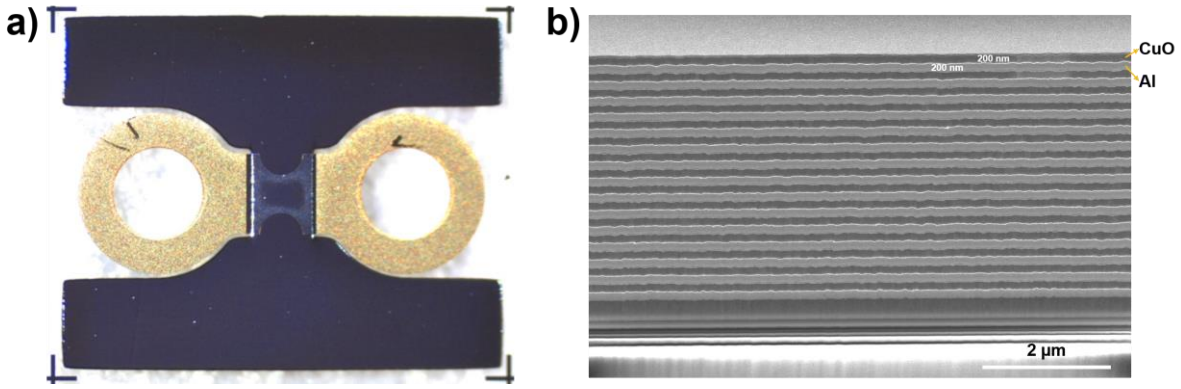

***Figure 4**. Digital image of one single RMFB chip (a) and SEM cross section image of 15 bilayers of CuO/Al 200 nm/200 nm reactive multilayer layers (b).*

2.2. Direct writing nanothermite films to fabricate the EMFB

Materials - The aluminum nanopowders (Al, average particle size: 80 nm; active content: 69 %) and titanium nanoparticles (Ti, average particle size: 70 nm; active content: 72%) were purchased from Novacentrix (USA) and US Research Nanomaterials (USA), respectively, and then stored in a glove box for future uses. Copper oxide (CuO, average particle size: 100 nm), copper nitrate trihydrate, 25% aqueous ammonia, ethanol (CH_3CH_2OH, anhydrous, 99.9%), polyvinylidene fluoride (PVDF), and dimethylformamide (99.9%) purchased from Merck (Germany) were directly used as received.

Inks preparation - To prepare energetic inks, 100 mg of PVDF was first dissolved in 3 mL DMF and stirred until a clear and transparent solution is formed; then a total amount of 900 mg of thermite powders, contain certain amount of Al, Ti, and CuO, were added the PVDF/DMF solution and stirred for 60 minutes followed by a sonication for 2 hours. The inks were stirred and sonicated for another 60 minutes before printing. The detailed information on inks preparation is summarized in **Table 2**. **Figure 5** shows optical and SEM images of as prepared Al/CuO/PVDF inks. As shown in the SEM images, both Al (irregular shape) and CuO (slightly bigger spherical shape) nanoparticles are well wrapped by PVDF binder. Besides, there are many micropores in the film that could be a result of the DMF solvent evaporation. The writing of the prepared inks was done using a volumetrically controlled dispenser developed in our lab. The details of this set-up can be found in our previous work [43].

***Table 2**. Chemical composition of the Al/Ti/CuO/PVDF energetic inks with different titanium loading.*

Energetic inks	Al (mg)	CuO (mg)	Ti (mg)	PVDF/DMF	Mol fraction of Ti in the fuel
Al/CuO/PVDF	260	640	0	100 mg / 3 mL	0
Al/Ti_30%/CuO/PVDF	168	634	116		0.3
Al/Ti_50%/CuO/PVDF	110	616	176		0.5
Al/Ti_70%/CuO/PVDF	62	608	230		0.7
Ti/CuO/PVDF	0	600	300		1

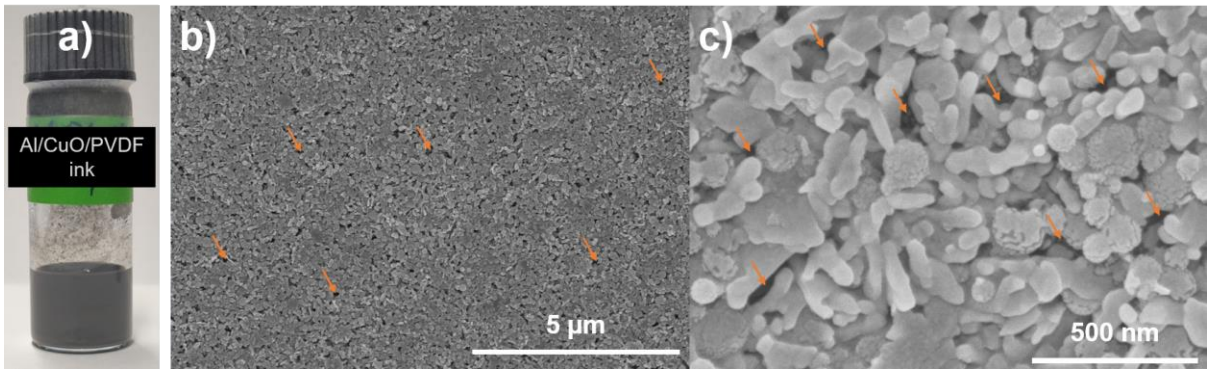

Figure 5. *Optical (a) and SEM (b-c) image of the Al/CuO/PVDF ink. The orange arrows indicate mark the location of the micro-pores.*

EMFB igniter fabrication - **Figure 6** summarizes the step-by-step fabrication process of a EMFB igniter. A 250 µm thick peripherical wall is built on the MFB and around the resistance serving as a chamber to store the energetic material and the shape of the wall is designed to be identical as to the RMF on EMFB igniters for a comparison purpose. Briefly describing the process, a 255 µm thick dry film (DF-SUEX 250, SU8 epoxy-based photoresist) was laminated onto the MFB chip by a laminator (Shipley 3024) with a rolling speed of 0.4 $m \cdot min^{-1}$, a rolling pressure of 1.5 bars, and a temperature of 85 °C. Then the DF coated MFB chip was exposed to UV light through a mask with the H-shaped pattern and followed by development to remove the extra DF part on the chip in order to obtain the chamber for the ink deposition. Then, the Al/Ti/CuO/PVDF inks were deposited into the designed container and the final EMFB igniter (step 4, **Figure 6**) is obtained after dying at 80 ºC for 60 minutes.

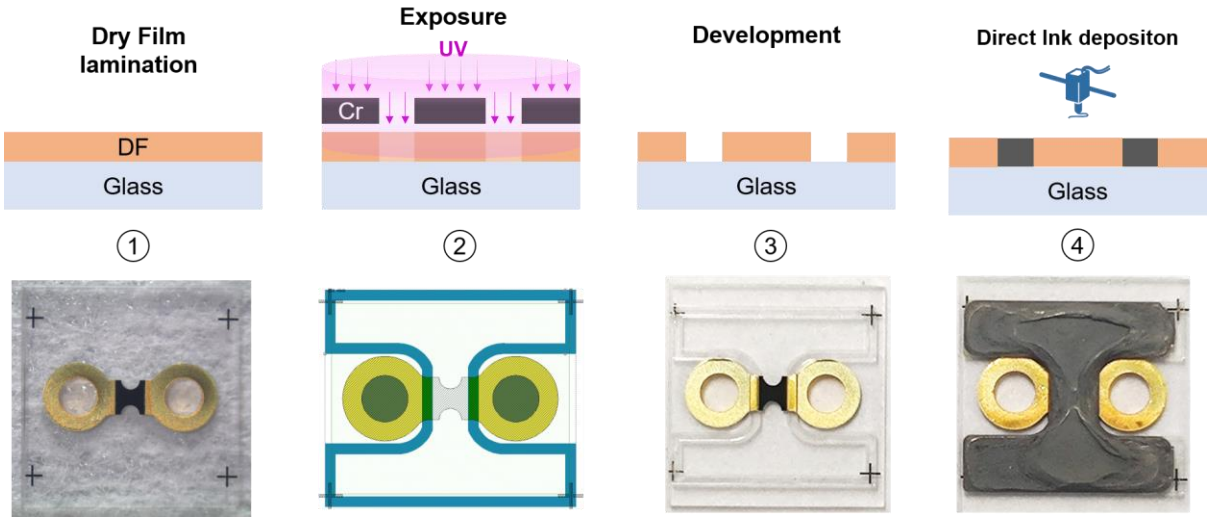

Figure 6. *Process flow of EMFB igniter fabrication.*

2.3. Characterization

Materials characterization - The morphological and interfacial analysis of the multilayers were carried out by Transmission Electron Microscopy (TEM), Scanning Transmission Electron Microscopy (STEM) using a JEOL cold-FEG JEM-ARM200F operated at 200 kV (energy resolution 0.3 eV) equipped with a probe Cs corrector reaching a spatial resolution of 0.078 nm. Elemental distribution and elemental mapping were obtained by energy-dispersive X-ray Spectroscopy (EDX) recorded on a JEOL CENTURIO SDD detector. Chemical composition of the interfacial layer was analyzed by electron energy-loss spectroscopy (EELS) obtained on a Gatan Imaging Filter Quantum using a dispersion of 0.5 eV/channel, a collection semi angle of 19.4 mrad and a convergence semi-angle of 14.8 mrad. The spatial resolution was estimated at 0.5 nm. STEM samples were prepared by Focused Ion Beam (FIB) technique on FEI Helios NanoLab DualBeam.

Ignition characterization - The multilayers were ignited under ambient conditions using externally applied direct current pulse through the Ti filament of the chips as presented in the previous works [37,45]. For each test, the current was adjusted so as to keep the same dissipated power (6.125 W). The ignition delay was measured using a photodiode (VISHAY, BPV10) biased at 5 V placed a few centimeters away from the sample and capable of detecting the optical flash emitted from the ignition event. A 1 kΩ dummy resistance was used to measure the photocurrent. All electrical signals were acquired on a digital oscilloscope and processed using in-house programs. Ten tests were performed

per sample configuration, and a mathematical average value of ignition delay (ms) was constituted. The ignition energy, calculated as the integral of power over time (up to initiation) was also calculated.

3. Results and discussions

3.1. RMFB ignition characteristics

Ti outperforms Cr as resistive filament in RMFB. **Figure 7** presents the optical emissions (photodiode signals) of RMBF igniters with different metal bridges (Ti and Cr) using reactive multilayer films made of 15 bilayers of CuO/Al, referred to as $(CuO/Al)_{15}$. **Table 3** summarizes their ignition characteristics. Both samples show a sharp emission profile with a similar flash intensity at ~ 2.2 indicating a similar flame temperature generated from the combustion of the $(CuO/Al)_{15}$ regardless of the resistive metal. Nonetheless, RMFB with a Ti bridge burns slightly faster (albeit highly dispersed) than the Cr counterpart, a phenomenon undoubtedly attributed to the higher roughness of the Cr surface, as illustrated in **Table 2**. Increased roughness results in a greater surface area. As salient observation, RMFB devices with Ti resistance filament features an ignition delay nearly 14 times faster than Cr resistance and an ignition energy ~7 times lower. Note that the interface between the metal bridge and the thermite multilayer is kept constant as the first layer is always 200 nm of CuO and the whole stack is also kept the same for both RMFB devices. Hence, the sole distinction between them lies in the type of resistive metal used.

Table 3*. Ignition characteristics of RMFB devices with two different resistive filaments*

RMBF	Ignition delay (ms)		Ignition energy (mJ)		Flash intensity (a.u.)		Burn time (ms)	
	Cr	Ti	Cr	Ti	Cr	Ti	Cr	Ti
$(CuO/Al)_{15}$	68 ± 14	5 ± 2	270 ± 47	39 ± 12	2.5 ± 0.1	2.2 ± 0.1	0.89 ± 0.10	0.72 ± 0.01

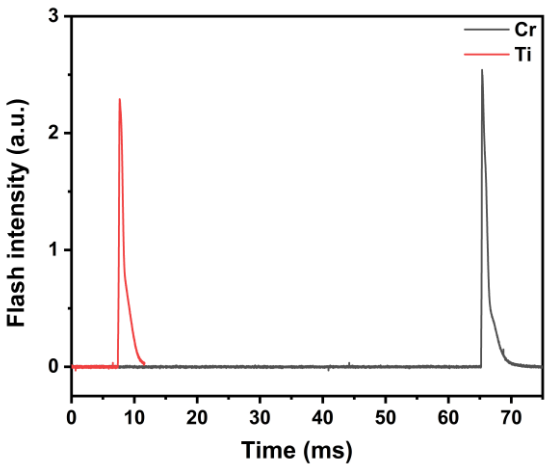

Figure 7. *Optical emission of $(CuO/Al)_{15}$-based RMFB igniters with different resistive filaments.*

To understand the cause for such difference in ignition delay between Cr and Ti, one needs to look at intrinsic properties of the material itself from both the physical heating and chemical point of views.

The temperature profiles upon resistive heating of the filaments were simulated using COMSOL Multiphysics and the results are presented in **Figure S2**. When a current of 1.75 A with a duration of 0.5 ms is applied to the resistive filament, both Cr and Ti show very similar temperature profile in the resistance, which might suggest a similar heating scenario for both metallic filaments. Thus, it is essential to evaluate if any chemical effects are involved in the ignition mechanism to account for the significant difference between the ignition delays of RMFB using Cr and Ti as the resistant filaments.

Chromium is less reactive than titanium and it has never been used as a fuel in thermite due to its passivated oxide layer. A thin, highly-dense chromium oxide is spontaneously formed at ambient which inhibits further oxygen diffusion towards to chromium and thus result in its low reactivity [46]. Rather, chromium oxide was used as a metal oxide coupled with aluminum to form energetic materials [47]. The ignition of Cr-based RMFB relies solely on Joule heating of the Cr bridge, whereas Ti-based RMFB ignition capitalizes on the high reactivity of Ti upon contact with oxygen sources or strong oxidizers like CuO [30,48], along with the significant exothermicity of its oxidation process.

In Ref [30], the reactivity of sputtered Ti/CuO thermite systems was investigated, unveiling that titania, the low density terminal reaction oxide, is a poor barrier to oxygen diffusion [30,48], unlike the case of alumina or chromium oxide. It grows and propagates into the titanium layer, driven by the diffusion

and reaction of oxygen atoms released by CuO at 300 °C [30]. Additional high-resolution electron microscopy and spectroscopy measurements revealed that the CuO/Ti redox reaction follows a two-step oxidation process: Titanium undergoes initial oxidation into TiO at 300 °C, followed by further oxidation into crystalline TiO_2 at 500 °C. This is why employing titanium as the metal bridge allows for a significant reduction in the electrical power required for ignition. In addition to the heat generated by the Joule effect, the oxidation of titanium at low temperatures contributes to the overall heat production.

To validate this hypothesis that Ti resistance might react with the first CuO layer from the reactive multilayer film, two bilayers of CuO/Al with thicknesses of 200/200 nm were deposited onto the Ti-based RMFB chip. A current of 1 A (2W) for a duration of 100 ms was applied to the bridge and a FIB lamella was prepared to observe the resulting chemical and morphological modification in the stack (**Figure S3**). On the SEM cross-section of **Figure 8a**, the five nanolayers are clearly identified: from bottom to the top, Ti resistance filament, CuO, Al, CuO, and Al nanolayer. Such layering structure is reconfirmed by the corresponding EDX mapping results as presented in **Figure 8b**. Following the application of current, we observe that reactions have occurred at all layers, resulting in significant changes in the morphology and thickness of each nanolayer (**Figure 8c).** Focusing on the Ti filament layer only, the EDX mapping (**Figure 8d**) clearly shows that Ti layer underwent oxidation: the thickness of Ti layer is increased from 290 nm to 315 nm before and after the current application. And the entire Ti layer has been oxidized to a certain extent with a clear TiO_x interfacial layer formed in between Ti and CuO nanolayer. The interfacial layer typically has a thickness ranging from 20 to 50 nm throughout its depth. The results confirm that the titanium bridge exothermically reacts with the first CuO layer and thus play favor the ignition process of EMFB. Titanium metal bridge is chosen as the resistive material for the rest of the study. Unless specified, MFB refers to Ti-based MFB in the following sections of this article.

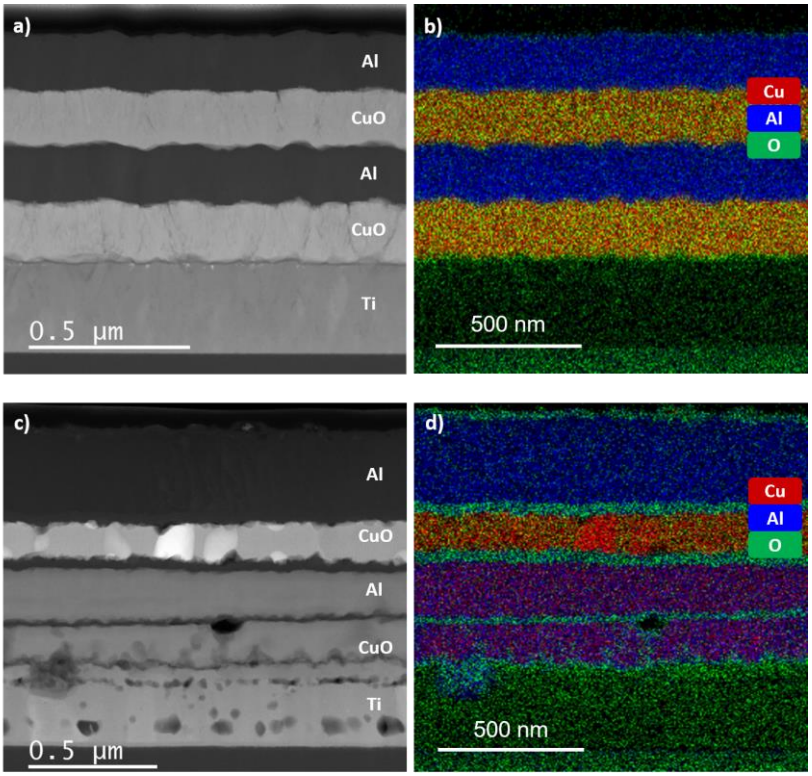

Figure 8*. TEM and EDX mapping of the multilayer before and after current application: 1 A (2 W), 100 ms).*

Fast response and low-energy input of RMFB igniter. Reducing ignition time can be achieved either by increasing the input current [28] which is not desirable in miniaturized and embedded systems, or, by modifying the composition or properties of the thermite film [30,37,38]. We explored the replacement of Al by Ti in the first bilayer of CuO/Al multilayer films owing to the high reactivity of Ti as a fuel [30,49]. $(CuO/Al)_{15}$ was employed as the reference sample. By replacing the first 1 CuO/Al bilayers with CuO/Ti, $(CuO/Ti)_1/(CuO/Al)_{14}$ powered RMFB igniter was fabricated. **Table 4** summarizes all the ignition characteristics (ignition delay/energy + flash intensity + burn time) for these two RMFB igniters and **Figure S4** shows their corresponding optical emission curves. Burn time was derived from full width at half maximum of the flash intensity curves shown in **Figure S4b**.

Noted that the values of all the ignition characteristics (except for flash intensity) are improved to varying degrees when Al is being replaced by Ti in the first thermite bilayer. Specifically, substituting the 1st CuO/Al bilayer by CuO/Ti, both ignition delay and ignition energy are improved by almost 5 times in comparison to $(CuO/Al)_{15}$, respectively; and burn time is reduced by 50%; On the other hand,

there was a slight negative modification in flash intensity, with a reduction of 0.1 which is neglectable. The as-reported reduced ignition delay and energy as well as burn time in this section is a direct reflection of high reactivity of CuO/Ti [30] compared to CuO/Al. The decreased flash intensity of (CuO/Ti)1/(CuO/Al)14 is likely attributable to the lower heat of reaction of CuO/Ti compared to CuO/Al: 2500 J/g against 4070 J/g.

This section demonstrates that solely adding 1 CuO/Ti bilayer prior to the deposition of CuO/Al multilayers leads to significant improving of ignition performance of RMFB igniters with only one disadvantage by modestly reducing the flash intensity, i.e. the flame temperature.

Table 4. *Ignition characteristics of $(CuO/Al)_{15}$ and $(CuO/Ti)_1/(CuO/Al)_{14}$ RMFB igniters*

RMFB igniters	Ignition delay (ms)	Ignition energy (mJ)	Flash intensity (a.u.)	Burn time (ms)
$(CuO/Al)_{15}$	5.1 ± 1.8	39.0 ± 12.3	2.2 ± 0.1	0.72 ± 0.01
$(CuO/Ti)_1/(CuO/Al)_{14}$	1.0 ± 0.6	7.8 ± 5.2	2.1 ± 0.1	0.37 ± 0.03

To enhance the flash intensity from the igniters, we propose replacing the sputter-deposited film with a thicker energetic layer deposited through writing techniques.

3.2. EMBF *vs.* RMBF ignition characteristics

As a reference, and to compare with RMBF on which 15 bilayers of Al/CuO is deposited, a conventional Al/CuO thermite couple was chosen and then dispersed in a PVDF/DMF solution to obtain the energetic Al/CuO/PVDF ink following by their direct writing onto MFB chips to fabricate EMFB igniters. For each device, ~3 mg of ink is deposited. The ignition performances are summarized in **Table 5**. After measurement, a total of ~3 mg of Al/CuO/PVDF energetic film was printed into the EMFB igniter.

From **Table 5**, we observe a huge difference between the burn time and flash intensity of RMFB and EMFB igniters: RMFB burns ~10 times faster than EMFB; however, EMFB flash is brighter than RMFB by almost 80% more. PVDF, employed as a binder in EMFB, may impede heat transfer from the resistive filament to the energetic materials during ignition. This results in a prolonged ignition delay and slower burn rate compared to the RMFB configuration. In RMFB, where dense reactive

multilayer films directly contact the resistive filament, ignition and propagation occur more efficiently [50]. The difference in flash intensity between the two types of igniter is due to the different loading of the energetic materials in igniters: RMFB typically contains approximately 0.35 mg of reactive multilayer films, while EMFB typically contains around 3 mg of energetic materials. Additionally, the presence of PVDF in the energetic ink may reduce heat loss to the environment as it happens in RMFB case [45], to some extent contributing to the higher flame temperature/flash intensity.

When comparing the Al/CuO/PVDF-based EMFB igniter with its Al/CuO RMFB counterpart, it demonstrates an ignition delay of 7 ms and an ignition energy of 56 mJ, which are nearly 30% lower than the values achieved with $(CuO/Al)_{15}$ powered RMFB igniters (**Table 4**). To improve its ignition performance, different amount of Ti nanoparticles (**Table 2**) were added into the Al/CuO/PVDF ink and meanwhile keeping the stoichiometric ratio unchanged as described in Experimental section. One EMBF containing a ink with only Ti/CuO/PVDF was also fabricated for comparison purpose.

The fabricated EMFB igniters with different titanium loading were tested for their ignition performance and the results are presented in **Table 5** and **Figure S5**. All Al/Ti/CuO/PVDF samples demonstrate flash intensities higher than 3.4 and burn time more than 4.3 ms except for the Ti/CuO/PVDF case, which features the lowest flash intensity (~2) and shortest burn time (~3 ms). The low flash intensity obtained for Ti/CuO/PVDF based EMFB is probably due to their lower flame temperature than Al/CuO [51]. It has been verified recently that the Ti/CuO undergoes a low-temperature condensed phase reaction as a result of lower flame temperature and flash intensity output [30].

It is noteworthy that Ti/CuO/PVDF exhibits the lowest ignition delay and shortest burn time, approximately at 2 and 3 ms. Previous works have reported that Ti/CuO burns 5 times faster than Al/CuO [30]. However, even with Ti incorporation EMBF still exhibits longer ignition delay and burn time compared to RMFB composed $(CuO/Ti)_1/(CuO/Al)_{14}$ (burn time of around 1 ms). Other than the poor heat transfer within the PVDF binder as discussed earlier, another possible cause could be the titanium fuel itself. Like other fuel particles, titanium nanoparticles used in the energetic ink contains an oxide shell due to inevitable oxidation during fabrication and about 72% of the as-received titanium

nanoparticles remains its metallic state for thermite reaction ; in contrast, titanium thin film obtained by physical vapor deposition is pure metal [30,49]. Both reasons elaborated here account for the limited beneficial effect on ignition performance by Ti nanoparticle addition.

***Table 5**. Ignition characteristics of Al/Ti/CuO/PVDF EMFB igniters with different titanium loading.*

EMFB igniters	Ignition delay (ms)	Ignition energy (mJ)	Flash intensity (a.u.)	Burn time (ms)
Al/CuO/PVDF	7.2 ± 0.1	56.2 ± 0.4	3.7 ± 0.2	4.9 ± 0.1
Al/Ti_30%/CuO/PVDF	2.5 ± 0.8	18.4 ± 5.6	3.8 ± 0.1	5.0 ± 1.0
Al/Ti_50%/CuO/PVDF	3.5 ± 0.7	25.4 ± 4.6	3.7 ± 0.2	4.5 ± 1.8
Al/Ti_70%/CuO/PVDF	3.8 ± 1.6	21.5 ± 8.6	3.4 ± 0.3	4.3 ± 1.5
Ti/CuO/PVDF	2 ± 0.3	14.0 ± 2.0	2.2 ± 0.4	3.1 ± 1.2

Although EMFB underperform RMFB, Al/Ti_30%/CuO/PVDF EMFB does provide the best compromise between ignition performance and energetic output (flash intensity and burn time). It offers an ignition delay ~2 ms with a required energy input below 20 mJ, which can be interested for certain applications with not critical requirement and low budget. Accordingly, Al/CuO/PVDF could be equally preferred as the DIW ink formula for the reason that aluminum nanoparticles cost much less than titanium nanoparticles and thus can reduce the over fabrication cost for applications with low budget.

Based on the results presented in previous sections, i.e. replacing 1 CuO/Al bilayer with CuO/Ti that is in contact with the Ti bridge leads to a very fast ignition (1 ms of ignition time), and a few mg of Al/CuO/PVDF thermites generates high flash intensity but suffer from long ignition delay, a new type of EMFB igniter powered by both reactive multilayers and energetic inks is investigated in the next section.

3.3. Towards a cost-effective and low-energy input EMFB igniter

Both PVD and DIW procedures are used to fabricate this new igniter: 1 bilayer of CuO/Ti was deposited on an MFB chip. Rather than stacking 14 bilayers CuO/Al reactive multilayer films upon as presented in section 3.1., an energetic ink composed of Al/CuO/PVDF is chosen as the replacement due to its high flame temperature and cost-effective fabrication process. **Table 6** summarize the ignition performance of all igniters, which are categorized in 3 groups of samples: Group A – RMFB igniters from Section 3.1; Group B – $(CuO/Ti)_1$/inks igniters and Group C – $(CuO/Ti)_5$/inks igniters.

With extra energetic Al/CuO/PVDF inks deposited on $(CuO/Ti)_1$ multilayer film, this new EMFB igniter presents an ignition delay at ~9 ms, which are much longer than $(CuO/Ti)_1/(CuO/Al)_{14}$ RMFB. As $(CuO/Ti)_1$ RMFB shows no ignition upon trigger and our group has reported that $(CuO/Ti)_5$ RMFB features an ignition delay at ~20 μs [30], we directly deposited energetic ink on top of $(CuO/Ti)_5$ to obtain $(CuO/Ti)_5$/ink EMFB. It features an ignition delay at ~0.68 ms and ignition energy at ~2 mJ, similar level as $(CuO/Ti)_5$ RMFB. It appears that the deposited energetic ink materials on CuO/Ti multilayer film does not pose much negative effect on the ignition readiness of the EMFB probably because the deposited inks are not in direct contact with the resistance and thus do not alter the dynamic between the resistance and $(CuO/Ti)_5$ film upon triggering.

Additionally, the flash intensity increased from 0.1 (without Al/CuO/PVDF) to around 3.9 (with Al/CuO/PVDF) owing to the extensively increased energetic materials loading (almost 25 times, from ~0.35 mg to ~3 mg). Upon triggering, $(CuO/Ti)_5$ quickly ignites and generated flame/heat then ignites the Al/CuO/PVDF film followed by a continues propagation within the printed materials. Thus, by combing the PVD and DIW techniques, this new igniter offers a competitive ignition performance and much faster fabrication process as oppose to MFB ignites powered solely by either reactive multilayer films or energetic inks.

***Table 6**. Ignition performance of EMFB igniters powered by CuO/Ti reactive multilayer films and Al/CuO/PVDF energetic inks.*

MFB igniters		Ignition delay (ms)	Ignition energy (mJ)	Flash intensity (a.u.)	Burn time (ms)
Group A	$(CuO/Ti)_1/(CuO/Al)_{14}$	1.0 ± 0.6	7.8 ± 5.2	2.1 ± 0.1	0.37 ± 0.03
	$(CuO/Al)_{15}$	5.1 ± 1.8	39.0 ± 12.3	2.2 ± 0.1	0.72 ± 0.01
Group B	$(CuO/Ti)_1$				
	$(CuO/Ti)_1$/inks	9.4 ± 2.2	77.3 ± 2	3.8 ± 0.2	6.1 ± 0.2
	Al/CuO/PVDF inks	7.2 ± 0.1	56.2 ± 0.4	3.7 ± 0.2	4.9 ± 0.1
Group C	$(CuO/Ti)_5$	0.02 ± 0.01	0.2 ± 0.1	0.1 ± 0.01	0.5 ± 0.2
	$(CuO/Ti)_5$/inks	0.68 ± 0.3	1.9 ± 0.6	3.9 ± 0.1	5.7 ± 0.7

4. Conclusions

In this work, we studied ignition characteristics of both chromium and titanium based MFB igniters by magnetron sputtering reactive thermite multilayer films onto the glass chips. Results show that titanium-based igniters feature ignition delay at least 4 times faster than the chromium-based ones. Atomically resolved microscopy and spectroscopy characterization results reveal the reason why titanium outperform chromium as a resistive filament is because titanium not just serves as a resistive filament to heat the energetic materials but also participate in the thermite reaction. The Ti resistance engages in a redox reaction with the first CuO layer that is in direct contact with and hence facilitate the ignition process giving a shorter ignition delay. Additionally, RMFB igniter featuring an extremely fast ignition (below 1 ms) is manufactured by inserting CuO/Ti multilayers into CuO/Al for applications requiring instant response. To reduce fabrication cycle time of RMFB and meanwhile retaining its ignition property, we designed and fabricated an EMFB igniter by taking advantages of both PVD and DIW techniques, i.e. a combination of reactive multilayer films (for fast ignition) and energetic inks (for higher energetic materials loading and energy output). Both aspects in EMFB igniters can be tuned by

either by changing the thermite types or altering the multilayer/ink ratio. By sealing the energetic materials in EMFB igniters with an encapsulation layer (nitrocellulose), these igniters can be stored in various environment for future uses with similar aging behaviours of energetic materials used in the industry [52]. This paper provides a novel approach of designing and fabricating micro igniters with great ignition performance and fast process time that can be used as the first chain of pyrotechnical devices to ignite a secondary pyrotechnical material.

CRediT authorship contribution statement

Tao Wu: Conceptualization, Methodology, Investigation, Formal analysis, Data curation, Visualization, Validation, Writing – original draft, Writing – review & editing; **Vidushi Singh**: Methodology, Investigation, Data curation, Validation, Writing – review & editing; **Baptiste Julien**: Methodology, Investigation, Formal analysis, Visualization, Validation, Writing – review & editing; **Maria-Isabel Mendoza-Diaz**: Methodology, Investigation, Validation; **Fabien Mesnilgrente**: Methodology, Resources, Validation; **Samuel Charlot**: Methodology, Resources, Validation; **Carole Rossi**: Conceptualization, Methodology, Supervision, Resources, Project administration, Funding acquisition, Writing – review & editing.

Funding Sources

C.R. received funding from the European Research Council (ERC) under the European Union's Horizon 2020 research and innovation program (grand agreement No. 832889 - PyroSafe).

Declaration of Competing Interests

The authors declare that they have no known competing financial interests or personal relationships that could have appeared to influence the work reported in this paper.

Acknowledgements

The authors grateful acknowledge support from the European Research Council (H2020 Excellent Science) Researcher Award (grant 832889 – PyroSafe). This work was also supported by LAAS-CNRS technology platform, a member of Renatech network. The authors also acknowledge the help from Teresa Hungria and Claudie Josse for TEM lamina preparations and observations.

Appendix A. Supplementary data

Supplementary data to this article can be found online at …

Data availability

Data will be made available on request.

REFERENCES

[1] C. Ru, J. Dai, J. Xu, Y. Ye, P. Zhu, R. Shen, Design and optimization of micro-semiconductor bridge used for solid propellant microthrusters array, Eur. Phys. J. Appl. Phys. 74 (2016) 30103. https://doi.org/10.1051/epjap/2016160003.

[2] S.M. Danali, R.S. Palaiah, K.C. Raha, Developments in Pyrotechnics (Review Paper), Def. Sci. J. 60 (2010) 152-158. https://doi.org/10.14429/dsj.60.333.

[3] E.-C. Koch, 2006–2008 Annual Review on Aerial Infrared Decoy Flares, Propellants Explos. Pyrotech. 34 (2009) 6–12. https://doi.org/10.1002/prep.200700219.

[4] H. Pezous, C. Rossi, M. Sanchez, F. Mathieu, X. Dollat, S. Charlot, L. Salvagnac, V. Conédéra, Integration of a MEMS based safe arm and fire device, Sens. Actuators Phys. 159 (2010) 157–167. https://doi.org/10.1016/j.sna.2010.03.017.

[5] C. Rosères, L. Courty, P. Gillard, C. Boulnois, Thermal Behaviour and Kinetic Parameters of Ternary Mg+SrO2+DNAN Pyrotechnic Compositions, Propellants Explos. Pyrotech. 47 (2022) e202100269. https://doi.org/10.1002/prep.202100269.

[6] X. Guo, T. Liang, Md.L. Islam, X. Chen, Z. Wang, Highly Reactive Thermite Energetic Materials: Preparation, Characterization, and Applications: A Review, Molecules 28 (2023) 2520. https://doi.org/10.3390/molecules28062520.

[7] Y. Chen, W. Ren, Z. Zheng, G. Wu, B. Hu, J. Chen, J. Wang, C. Yu, K. Ma, X. Zhou, W. Zhang, Reactivity adjustment from the contact extent between CuO and Al phases in nanothermites, Chem. Eng. J. 402 (2020) 126288. https://doi.org/10.1016/j.cej.2020.126288.

[8] W. He, W. Ao, G. Yang, Z. Yang, Z. Guo, P.-J. Liu, Q.-L. Yan, Metastable energetic nanocomposites of MOF-activated aluminum featured with multi-level energy releases, Chem. Eng. J. 381 (2020) 122623. https://doi.org/10.1016/j.cej.2019.122623.

[9] T. Wu, F. Sevely, B. Julien, F. Sodre, J. Cure, C. Tenailleau, A. Esteve, C. Rossi, New coordination complexes-based gas-generating energetic composites, Combust. Flame 219 (2020) 478–487. https://doi.org/10.1016/j.combustflame.2020.05.022.

[10] L. Glavier, A. Nicollet, F. Jouot, B. Martin, J. Barberon, L. Renaud, C. Rossi, Nanothermite/RDX-Based Miniature Device for Impact Ignition of High Explosives, Propellants Explos. Pyrotech. 42 (2017) 308–317. https://doi.org/10.1002/prep.201600154.

[11] G.A. Ardila Rodríguez, S. Suhard, C. Rossi, D. Estève, P. Fau, S. Sabo-Etienne, A.F. Mingotaud, M. Mauzac, B. Chaudret, A microactuator based on the decomposition of an energetic material for disposable lab-on-chip applications: fabrication and test, J. Micromechanics Microengineering 19 (2008) 015006. https://doi.org/10.1088/0960-1317/19/1/015006.

[12] H. Yang, Z. Qiao, W. Wang, P. Tang, S. Man, X. Li, Y. Xie, D. Tang, X. Li, G. Yang, Self-destructive microchip: Support-free energetic film of BiOBr/Al/Bi2O3 nanothermites and its destructive performance, Chem. Eng. J. 459 (2023) 141506. https://doi.org/10.1016/j.cej.2023.141506.

[13] A. Nicollet, L. Salvagnac, V. Baijot, A. Estève, C. Rossi, Fast circuit breaker based on integration of Al/CuO nanothermites, Sens. Actuators Phys. 273 (2018) 249–255. https://doi.org/10.1016/j.sna.2018.02.044.

[14] F. Sevely, T. Wu, F.S. Ferreira de Sousa, L. Seguier, V. Brossa, S. Charlot, A. Esteve, C. Rossi, Developing a highly responsive miniaturized security device based on a printed copper ammine energetic composite, Sens. Actuators Phys. 346 (2022) 113838. https://doi.org/10.1016/j.sna.2022.113838.
[15] S.S. Pandey, N. Banerjee, Y. Xie, C.H. Mastrangelo, Self-Destructing Secured Microchips by On-Chip Triggered Energetic and Corrosive Attacks for Transient Electronics, Adv. Mater. Technol. 3 (2018) 1800044. https://doi.org/10.1002/admt.201800044.
[16] J.-R. Lee, C.C. Chia, C.-W. Kong, Review of pyroshock wave measurement and simulation for space systems, Measurement 45 (2012) 631–642. https://doi.org/10.1016/j.measurement.2011.12.011.
[17] M. Baloochi, D. Shekhawat, S.S. Riegler, S. Matthes, M. Glaser, P. Schaaf, J.P. Bergmann, I. Gallino, J. Pezoldt, Influence of Initial Temperature and Convective Heat Loss on the Self-Propagating Reaction in Al/Ni Multilayer Foils, Materials 14 (2021) 7815. https://doi.org/10.3390/ma14247815.
[18] A.J. Swiston, E. Besnoin, A. Duckham, O.M. Knio, T.P. Weihs, T.C. Hufnagel, Thermal and microstructural effects of welding metallic glasses by self-propagating reactions in multilayer foils, Acta Mater. 53 (2005) 3713–3719. https://doi.org/10.1016/j.actamat.2005.04.030.
[19] D.M.B. Dombroski, A. Wang, J.Z. Wen, M. Alfano, Joining and welding with a nanothermite and exothermic bonding using reactive multi-nanolayers – A review, J. Manuf. Process. 75 (2022) 280–300. https://doi.org/10.1016/j.jmapro.2021.12.056.
[20] H. Sui, N. Huda, Z. Shen, J.Z. Wen, Al–NiO energetic composites as heat source for joining silicon wafer, J. Mater. Process. Technol. 279 (2020) 116572. https://doi.org/10.1016/j.jmatprotec.2019.116572.
[21] K.M. de Souza, M.J.S. de Lemos, R. dos R. Ribeiro, P.G.C. Martins, L.H. Gouvêa, Experimental and numerical investigation of the effect of alumina on thermite reation propagation for thermal plug and abandonment of oil wells, Int. J. Heat Mass Transf. 224 (2024) 125327. https://doi.org/10.1016/j.ijheatmasstransfer.2024.125327.
[22] R. Xie, X. Ren, L. Liu, Y. Xue, D. Fu, R. Zhang, Research on design and firing performance of Si-based detonator, Def. Technol. 10 (2014) 34–39. https://doi.org/10.1016/j.dt.2014.01.002.
[23] C. Rossi, R. Shen, Miniaturized Pyrotechnic Systems Meet the Performance Needs While Limiting the Environmental Impact, Micromachines 13 (2022) 376. https://doi.org/10.3390/mi13030376.
[24] K.-N. Lee, M.-I. Park, S.-H. Choi, C.-O. Park, H.S. Uhm, Characteristics of plasma generated by polysilicon semiconductor bridge (SCB), Sens. Actuators Phys. 96 (2002) 252–257. https://doi.org/10.1016/S0924-4247(01)00836-6.
[25] D.A. Benson, M.E. Larsen, A.M. Renlund, W.M. Trott, R.W. Bickes Jr., Semiconductor bridge: A plasma generator for the ignition of explosives, J. Appl. Phys. 62 (1987) 1622–1632. https://doi.org/10.1063/1.339586.
[26] K.L. Zhang, S.K. Chou, S.S. Ang, X.S. Tang, A MEMS-based solid propellant microthruster with Au/Ti igniter, SSSAMW 04 122 (2005) 113–123. https://doi.org/10.1016/j.sna.2005.04.021.
[27] J. Xu, Y. Tai, Y. Shen, J. Dai, W. Xu, Y. Ye, R. Shen, Y. Hu, Characteristics of energetic semiconductor bridge initiator based on different stoichiometric ratios of Al/MoO3 reactive multilayer films under capacitor discharge conditions, Sens. Actuators Phys. 296 (2019) 241–248. https://doi.org/10.1016/j.sna.2019.07.015.
[28] A. Nicollet, G. Lahiner, A. Belisario, S. Souleille, M. Djafari-Rouhani, A. Estève, C. Rossi, Investigation of Al/CuO multilayered thermite ignition, J. Appl. Phys. 121 (2017) 034503. https://doi.org/10.1063/1.4974288.
[29] V. Singh, B. JULIEN, L. Salvagnac, S. Pelloquin, T. Hungria, C. Josse, M. Belhaj, C. Rossi, Influence of process parameters on energetic properties of sputter-deposited Al/CuO reactive multilayers, Nanotechnology 33 (2022) 465704. http://iopscience.iop.org/article/10.1088/1361-6528/ac85c5.
[30] T. Wu, V. Singh, B. Julien, C. Tenailleau, A. Estève, C. Rossi, Pioneering insights into the superior performance of titanium as a fuel in energetic materials, Chem. Eng. J. 453 (2023) 139922. https://doi.org/10.1016/j.cej.2022.139922.

[31] C. Rossi, Engineering of Al/CuO Reactive Multilayer Thin Films for Tunable Initiation and Actuation, Propellants Explos. Pyrotech. 44 (2019) 94–108. https://doi.org/10.1002/prep.201800045.
[32] S. Fu, R. Shen, P. Zhu, Y. Ye, Metal–interlayer–metal structured initiator containing Al/CuO reactive multilayer films that exhibits improved ignition properties, Sens. Actuators Phys. 292 (2019) 198–204. https://doi.org/10.1016/j.sna.2019.04.019.
[33] H. Wang, B. Julien, D.J. Kline, Z. Alibay, M.C. Rehwoldt, C. Rossi, M.R. Zachariah, Probing the Reaction Zone of Nanolaminates at ∼μs Time and ∼μm Spatial Resolution, J. Phys. Chem. C 124 (2020) 13679–13687. https://doi.org/10.1021/acs.jpcc.0c01647.
[34] B. Bao, N. Yan, Y. Jiang, G. Wang, W. Ding, Temperature measurements and multi-physical field simulations of micro-sized metal film bridge, Appl. Therm. Eng. 104 (2016) 121–128. https://doi.org/10.1016/j.applthermaleng.2016.05.052.
[35] Y. Yan, W. Shi, H. Jiang, J. Xiong, W. Zhang, Y. Li, Characteristics of the Energetic Igniters Through Integrating Al/NiO Nanolaminates on Cr Film Bridge, Nanoscale Res. Lett. 10 (2015) 504. https://doi.org/10.1186/s11671-015-1204-9.
[36] J. Zapata, A. Nicollet, B. Julien, G. Lahiner, A. Esteve, C. Rossi, Self-propagating combustion of sputter-deposited Al/CuO nanolaminates, Combust. Flame 205 (2019) 389–396. https://doi.org/10.1016/j.combustflame.2019.04.031.
[37] V. Singh, T. Wu, E. Hagen, L. Salvagnac, C. Tenailleau, A. Estéve, M.R. Zachariah, C. Rossi, How positioning of a hard ceramic TiB2 layer in Al/CuO multilayers can regulate the overall energy release behavior, Fuel 349 (2023) 128599. https://doi.org/10.1016/j.fuel.2023.128599.
[38] V. Singh, T. Wu, L. Salvagnac, A. Estève, C. Rossi, Ignition and Combustion Characteristics of Al/TiB2-Based Nanothermites: Effect of Bifuel Distribution, ACS Appl. Nano Mater. 7 (2024) 3977–3987. https://doi.org/10.1021/acsanm.3c05578.
[39] J. Wang, Y. Li, B. Zhou, Z. Gao, Firing process and spectrum diagnosis of semiconductor bridge for high output energy micro-initiator, Sens. Actuators Phys. 270 (2018) 108–117. https://doi.org/10.1016/j.sna.2017.12.039.
[40] A. Nicollet, L. Salvagnac, V. Baijot, A. Estève, C. Rossi, Fast circuit breaker based on integration of Al/CuO nanothermites, Sens. Actuators Phys. 273 (2018) 249–255. https://doi.org/10.1016/j.sna.2018.02.044.
[41] B. Julien, J. Cure, L. Salvagnac, C. Josse, A. Esteve, C. Rossi, Integration of Gold Nanoparticles to Modulate the Ignitability of Nanothermite Films, ACS Appl. Nano Mater. 3 (2020) 2562–2572. https://doi.org/10.1021/acsanm.9b02619.
[42] S.C. Ligon, R. Liska, J. Stampfl, M. Gurr, R. Mülhaupt, Polymers for 3D Printing and Customized Additive Manufacturing, Chem. Rev. 117 (2017) 10212–10290. https://doi.org/10.1021/acs.chemrev.7b00074.
[43] F. Sevely, X. Liu, T. Wu, F. Mesnilgrente, B. Franc, S. Assie-Souleille, X. Dollat, C. Rossi, Effect of Process Parameters on the Properties of Direct Written Gas-Generating Reactive Layers, ACS Appl. Polym. Mater. 3 (2021) 3972–3980. https://doi.org/10.1021/acsapm.1c00513.
[44] R.R. Nellums, S.F. Son, L.J. Groven, Preparation and Characterization of Aqueous Nanothermite Inks for Direct Deposition on SCB Initiators, Propellants Explos. Pyrotech. 39 (2014) 463–470. https://doi.org/10.1002/prep.201400013.
[45] T. Wu, B. Julien, H. Wang, S. Pelloquin, A. Esteve, M.R. Zachariah, C. Rossi, Engineered Porosity-Induced Burn Rate Enhancement in Dense Al/CuO Nanothermites, ACS Appl. Energy Mater. 5 (2022) 3189–3198. https://doi.org/10.1021/acsaem.1c03805.
[46] P. Gibot, Templated synthesis of Cr2O3 material for energetic composites with high performance, Solid State Sci. 94 (2019) 162–167. https://doi.org/10.1016/j.solidstatesciences.2019.05.014.
[47] P. Gibot, M. Comet, A. Eichhorn, F. Schnell, O. Muller, F. Ciszek, Y. Boehrer, D. Spitzer, Highly Insensitive/Reactive Thermite Prepared from Cr2O3 Nanoparticles, Propellants Explos. Pyrotech. 36 (2011) 80–87. https://doi.org/10.1002/prep.201000080.
[48] H. Jabraoui, A. Estève, S. Hong, C. Rossi, Initial stage of titanium oxidation in Ti/CuO thermites: a molecular dynamics study using ReaxFF forcefields, Phys. Chem. Chem. Phys. 25 (2023) 11268–11277. https://doi.org/10.1039/D3CP00032J.

[49] W. Zhao, H. Wang, D.J. Kline, X. Wang, T. Wu, J. Xu, H. Ren, M.R. Zachariah, Influence of titanium addition on performance of boron-based thermites, Chem. Eng. J. 438 (2022) 134837. https://doi.org/10.1016/j.cej.2022.134837.
[50] H. Wang, M. Rehwoldt, D.J. Kline, T. Wu, P. Wang, M.R. Zachariah, Comparison study of the ignition and combustion characteristics of directly-written Al/PVDF, Al/Viton and Al/THV composites, Combust. Flame 201 (2019) 181–186. https://doi.org/10.1016/j.combustflame.2018.12.031.
[51] S.H. Fischer, M.C. Grubelich, Theoretical energy release of thermites, intermetallics, and combustible metals, in: Monterey, CA, USA, 1998. https://doi.org/10.2172/658208.
[52] T. Wu, G. Lahiner, C. Tenailleau, B. Reig, T. Hungria, A. Esteve, C. Rossi, Unexpected Enhanced Reactivity of Aluminized Nanothermites by Accelerated Aging, Chem. Eng. J. (2021) 129432. https://doi.org/10.1016/j.cej.2021.129432.